Synergistic TRAIL Sensitizers from *Barleria alluaudii* and *Diospyros maritima*

Emily L. Whitson,[†] Han Sun,[‡] Cheryl L. Thomas,[†] Curtis J. Henrich,[†,§] Thomas J. Sayers,[⊥,§] James B. McMahon,[†] Christian Griesinger,[‡] and Tawnya C. McKee*,[†]

[†]Molecular Targets Laboratory, Molecular Discovery Program, Center for Cancer Research, NCI-Frederick, Frederick, Maryland 21702, United States

[‡]Department of NMR Based Structural Biology, Max Planck Institute for Biophysical Chemistry, Am Fassberg 11, 37077 Göttingen, Germany
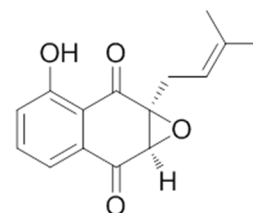
[§]SAIC-Frederick, Inc., Frederick, Maryland 21702, United States

[⊥]Laboratory of Experimental Immunology, Cancer and Inflammation Program, Center for Cancer Research, NCI-Frederick, Frederick, Maryland 21702, United States

S *Supporting Information*
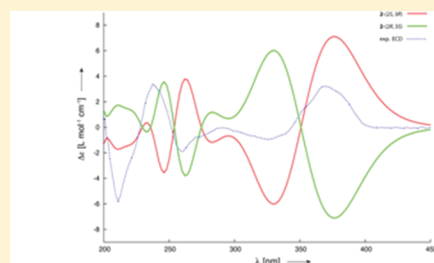
Calculated ECD vs. Experimental ECD → Absolute configuration

ABSTRACT: *Barleria alluaudii* and *Diospyros maritima* were both investigated as part of an ongoing search for synergistic TRAIL (tumor necrosis factor-α-related apoptosis-inducing ligand) sensitizers. As a result of this study, two naphthoquinone epoxides, 2,3-epoxy-2,3-dihydrolapachol (1) and 2,3-epoxy-2,3-dihydro-8-hydroxylapachol (2), both not previously isolated from natural sources, and the known 2-methylanthraquinone (3) were identified from *B. alluaudii*. Time-dependent density functional theory (TD-DFT) calculations of electronic circular dichroism (ECD) spectra were utilized to establish the absolute configuration of 1 and 2. Additionally, five known naphthoquinone derivatives, maritinone (4), ellipitinone (5), plumbagin (6), (+)-*cis*-isoshinanolone (7), and ethylidene-6,6′-biplumbagin (8), were isolated from *D. maritima*. Compounds 1, 2, and 4−6 showed varying levels of synergy with TRAIL. Maritinone (4) and ellipitinone (5) showed the highest synergistic effect, with more than a 3-fold increase in activity observed with TRAIL than with compound alone.

Tumor necrosis factor-α-related apoptosis-inducing ligand (TRAIL/Apo2L) is a member of the tumor necrosis factor (TNF) family of apoptosis-triggering proteins.[1] TRAIL promotes recruitment of the adaptor protein FADD (Fas-associated death domain) upon binding to death domain-containing transmembrane receptors, death receptors 4 and 5 (DR4, DR5). FADD is responsible for recruiting procaspase-8 and procaspase-10, which results in the formation of a trimerized receptor−ligand complex called DISC (death-inducing signaling complex). The activated initiator caspase-8 then activates effector caspase-3, caspase-6, and caspase-7, which triggers the caspase cascade and subsequently results in apoptosis.[2,3] In type I cancer cells, caspase-8 can directly activate downstream effector caspases to promote apoptosis. However, in type II cancer cells, apoptosis proceeds through cross-talk between the extrinsic and intrinsic pathways and involves the participation of the mitochondria.[4] TRAIL is

particularly important because it selectively induces apoptosis in cancer cells, while showing little to no effect in normal cells.[1,5] However, TRAIL resistance has been widely documented,[5−9] and there is evidence to suggest that combination chemotherapy regimens may be more effective than traditional cytotoxic monochemotherapy.[10−12] In this manner, TRAIL activity may be restored by sensitizing tumor cells with certain chemical agents. Therefore, a high-throughput screen was developed to identify compounds that could sensitize tumor cells to the killing effects of TRAIL.[5] As a result of this screen, we reported previously eight new clerodane diterpenes isolated from *Casearia arguta* with varying

levels of TRAIL synergy.[13] Here we describe the isolation and structure elucidation of two naphthoquinone epoxides from *Barleria alluaudii* as well as six known quinones from both *B. alluaudii* and *Diospyros maritima*, and their TRAIL-sensitizing activity.

■ RESULTS AND DISCUSSION

Bioassay-guided fractionation of the organic-soluble extracts of *B. alluaudii* and *D. maritima*, utilizing normal-phase chromatography, size-exclusion chromatography, and reversed-phase HPLC, resulted in the isolation of two naphthoquinone epoxides, 2,3-epoxy-2,3-dihydrolapachol (**1**) and 2,3-epoxy-2,3-dihydro-8-hydroxylapachol (**2**), as well as six known compounds (**3−8**).

1 R = H
2 R = OH
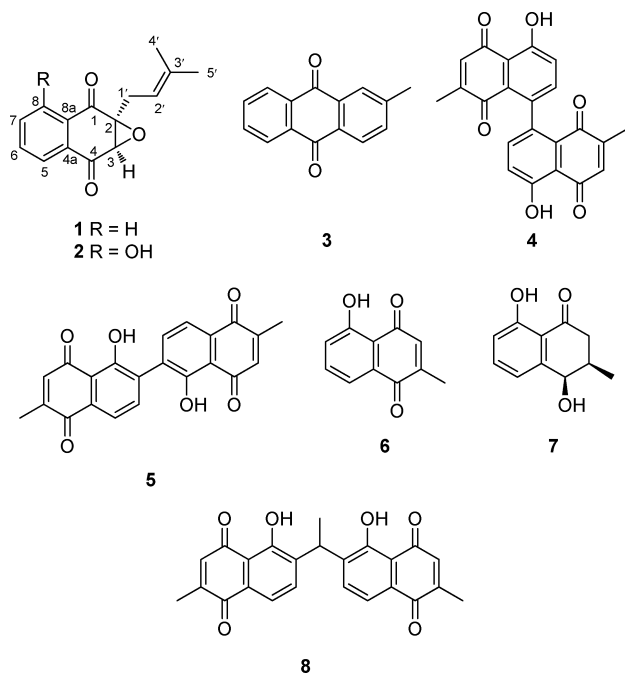
The molecular formula for **1**, C$_{15}$H$_{14}$O$_3$, was derived from NMR data (Table 1) and the HRESIMS ion at *m/z* 243.1020 ([M + H]$^+$; Δ +1.65 ppm). 1D- and 2D-NMR studies were utilized to establish the structure of **1**. Initial interpretation of the NMR data (Table 1) indicated that **1** contains six quaternary carbons, six methines, one methylene, and two methyls. The NMR data suggested this compound was a substituted naphthoquinone, with a 3-methyl-2-butenyl moiety and a one-proton singlet (δ$_H$ 3.83). The identity of **1** was established as 2,3-epoxy-2,3-dihydrolapachol (or 2-(3′-methyl-2′-butenyl)-2,3-epoxy-1,4-naphthoquinone) upon comparison of spectroscopic data with those reported in the literature.[14−17] This is the first reported incidence of **1** as a natural product, although it has been produced by total synthesis[14−16] and semisynthetically from 2-(3′-methyl-2′-buteny1)-2,3-epoxy-1,4-naphthalenedione-4,4-dimethoxy ketal.[17]

The molecular formula for **2**, C$_{15}$H$_{14}$O$_4$, derived from the HRESIMS ion at *m/z* 259.0966 ([M + H]$^+$; Δ +0.39 ppm) indicated that **2** contains one oxygen atom more than **1**. Initial interpretation of the NMR data (Table 1) indicated that **2** contains seven quaternary carbons, five methines, one methylene, and two methyls. The dispersion of the aromatic signals and the appearance of a broad OH singlet (δ$_H$ 11.39) suggested the addition of a hydroxy substituent on the aromatic

Table 1. NMR Data for 1 and 2 in CDCl$_3$

	1		**2**		
position	δ$_C$	δ$_H$, mult (*J*, Hz)	δ$_C$	δ$_H$, mult (*J*, Hz)	HMBC
1	192.0		197.3		
2	63.8		63.6		
3	59.2	3.83, s	59.1	3.79, s	2, 4, 4a, 1′
4	192.3		191.1		
4a	132.1		132.4		
5	127.0	7.92, ddd (7.1, 2.1, 0.8)	119.2	7.44, dd (7.5, 0.9)	1, 4, 6, 7, 8, 8a
6	134.5	7.72, ddd (7.5, 7.1, 2.1)	137.1	7.55, dd (8.4, 7.5)	4, 4a, 5, 7, 8, 8a
7	134.7	7.72, ddd (7.5, 7.1, 2.1)	124.7	7.18, dd (8.4, 0.9)	1, 4a, 5, 6, 8, 8a
8	127.7	8.00, ddd (7.1, 2.1, 0.8)	162.1		
8a	132.6		114.7		
1a′	26.4	3.02, dd (15.4, 8.1)	26.0	3.04, dd (15.3, 8.1)	1, 2, 3, 2′, 3′
1b′		2.66, dd (15.4, 6.9)		2.58, dd (15.3, 6.8)	1, 2, 3, 2′, 3′
2′	115.6	5.06, ddq (8.1, 6.9, 1.0)	115.2	5.01, ddq (8.1, 6.8, 1.0)	2, 3, 3′, 4′, 5′
3′	137.5		137.7		
4′	18.3	1.66, brs	18.2	1.63, brs	2′, 3′, 4′
5′	26.1	1.70, brs	26.1	1.68, brs	2′, 3′, 5′
OH-8				11.39, brs	

ring. Furthermore, the downfield shift of the phenol proton signal indicated that the proton is hydrogen bonded to the quinone oxygen. HMBC data (H-5/C-8; H-6/C-8; H-7/C-8) indicated the hydroxy group to be located at C-8. The identity of **2** was established as 2,3-epoxy-2,3-dihydro-8-hydroxylapachol (or 2-(3′-methyl-2′-butenyl)-2,3-epoxy-8-hydroxy-1,4-naphthoquinone) upon comparison of MS and ^{1}H NMR data with that of a reported intermediate in the synthesis of α-caryopterone.[18] Compound **2** has also not been reported as a natural product previously.

The absolute configuration of the naturally occurring epoxy naphthoquinone **2** was established by comparison of the observed electronic circular dichroism (ECD) spectrum with time-dependent density functional theory (TD-DFT)-calculated ECD spectra.[19,20] A conformational search using molecular mechanics calculations yielded 14 possible conformers within a 10 kcal/mol energy threshold. The geometries of **2** were optimized at the B3LYP/6-31G(d) level, affording six possible conformers within a 1 kcal/mol energy difference (**2a−2f**, Figure 1). The relative energies, relative zero-point energies, relative Gibbs free energies, and their respective conformational distributions are given in Table 2. The ECD calculations for **2a−2f** were then conducted with the B3LYP-6-31G(d) basis set using the IEFPCM solvent continuum model with methanol as the solvent. The calculated ECD spectra, weighted based on the Gibbs free energy, of both the 2*S*,3*R* and 2*R*,3*S* enantiomers are shown in Figure 2, along with the experimental ECD for **2**. The weighted ECD spectra for the 2*S*,3*R* enantiomer is in good accordance with the experimental ECD. In particular, the positive Cotton effect at 380 nm and the negative Cotton effect at 330 nm clearly follow the ECD pattern for **2**. Comparison between the experimental and calculated optical rotary dispersion (ORD) values for both possible enantiomers using DFT at three different wavelengths further supports the 2*S*,3*R* configuration (Figure S2, Table S3).
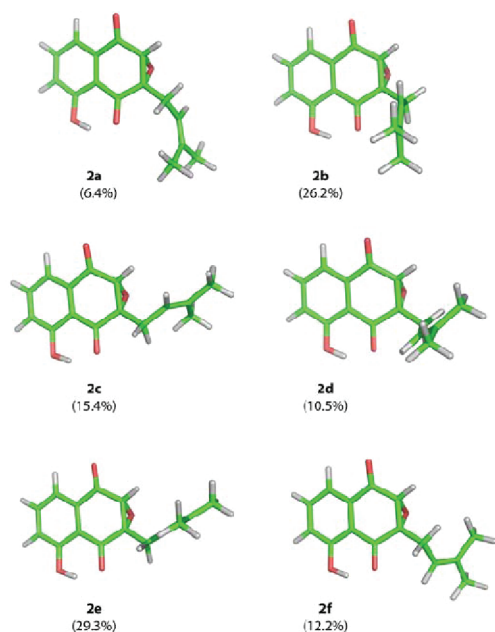
Figure 1. Six lowest energy conformers of (2S,3R)-2,3-epoxy-2,3-dihydro-8-hydroxylapachol (2). Conformer populations were calculated using the Gibbs free energy.

Table 2. Conformational Analysis of 2 Using the IEFPCM Solvent Continuum Model (Methanol)

conformer	ΔE^a	P_E (%)^b	$\Delta E_0{}^a$	P_{E0} (%)^b	ΔG^a	P_G (%)^b
2a	1.02	5.0	1.33	3.1	0.89	6.4
2b	0.05	25.9	0.04	27.4	0.07	26.2
2c	0.38	14.8	0.37	15.7	0.38	15.4
2d	0.21	19.7	0.30	17.8	0.61	10.5
2e	0	28.2	0	29.3	0	29.3
2f	0.88	6.4	0.87	6.7	0.52	12.2

^{a}Relative energy, relative zero-point energy, and relative Gibbs free energy at the B3LYP/6-31G(d) level, respectively (kcal/mol). ^{b}Conformational distribution calculated by using the respective parameters above at the B3LYP/6-31G(d) level.
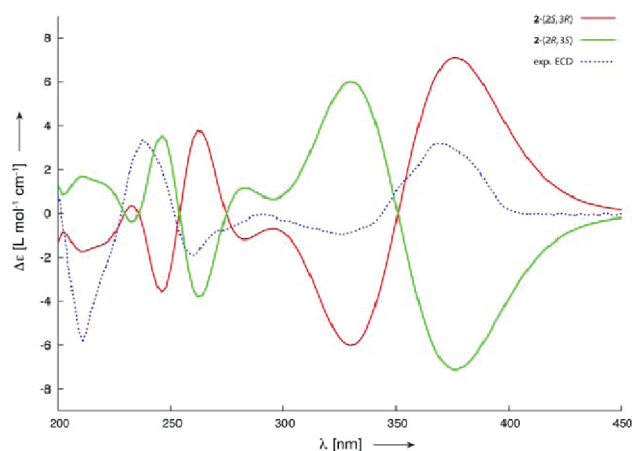

Figure 2. Comparison of experimental ECD values with those calculated for the two possible enantiomers (2S,3R and 2R,3S) of **2**. The calculations were performed with DFT at the B3LYP/6-31G(d) level using the IEFPCM solvent continuum model with methanol as the solvent. The calculated ECD values are weighted based on the Gibbs free energy.

Therefore, the absolute configuration of **2** was established as (2S,3R)-2,3-epoxy-2,3-dihydro-8-hydroxylapachol.

The absolute configuration of **1** was established by comparison of experimental and TD-DFT-calculated ECD spectra. Following the approach outlined above, geometry optimization of **1** resulted in six possible conformers within a 1 kcal/mol energy difference (**1a−1f**, Figure S3). A comparison of the observed ECD spectrum for **1** with spectra calculated by TD-DFT for the 2S,3R-**1** and 2R,3S-**1** enantiomers is seen in Figure 3. The weighted ECD spectra for the 2S,3R enantiomer is in good accordance with the experimental ECD for **1**. Interestingly, the optical rotations for compounds **1** and **2** are of opposite sign (**1**, −9.0; **2**, +92.8). Compound **1** was subjected to chiral HPLC analysis to determine whether a mixture of enantiomers was present, and a single peak was observed on six chiral columns (Supporting Information). The ORD values for the 2S,3R-**1** and 2R,3S-**1** enantiomers were also calculated using DFT at three different wavelengths. The ORD values for **1a−1f** are highly divergent, with half being of the opposite sign. Consequently, a small error in the energy calculation could result in an average ORD of the wrong sign. This is in contrast to the calculations for **2a−2f**, where only one conformer was the opposite sign. In a similar case, the correct ensemble with an accurate population approximating the full conformational space of the molecule was essential for calculating the chiroptical properties.[21] Furthermore, according to McCann and Stephens, the ORD values are not reliable if the absolute value of the difference between calculated and experimental for both enantiomers is less than 74.0.[23] Therefore, in the case of compound **1**, the conformational averaged $[\alpha]_D$ for the two enantiomers is ±28.9 and cannot be considered a reliable predictor of absolute configuration. Taken together with the good agreement between the 2S,3R-**1** calculated and experimental ECD spectra, biosynthetic principles support **1** having the same 2S,3R absolute configuration, given that **1** and **2** were concurrently isolated from the same organism. Therefore, a 2S,3R configuration is also proposed for **1**.

Compounds **3−8** were found to be 2-methylanthraquinone (tectoquinone) (**3**),[24,25] maritinone (**4**),[26,27] elliptinone (**5**),[28,29] plumbagin (**6**),[27,30] (+)-cis-isoshinanolone (**7**),[26,31] and ethylidene-6,6′-biplumbagin (**8**)[32,33] by comparison of their NMR and MS data with those in the literature. The relative configuration of cis-isoshinanolone (**7**) was supported by the small coupling constant observed between H-3 and H-4 (J = 2.8 Hz); cis and trans isomers show significantly different coupling constants (cis: J = 2.5 Hz; trans: J = 7.5 Hz).[26,31] The absolute configuration (3R,4R) was established by comparison of the ECD spectrum measured for **7** with those of the two possible enantiomers.[31]

ACHN cells are not sensitive to recombinant TRAIL ligand at concentrations up to 10 μg/mL, but they can be sensitized with pre-exposure to certain chemical sensitizers (e.g., the proteasome inhibitor bortezomib).[5] The TRAIL activities of compounds **1−8** are summarized in Table 3. Compounds **1**, **2**, and **4−6** fall into the "synergistic/toxic" category that has been previously described.[5] They have some toxicity alone, but synergize with TRAIL to kill cells (greater than an additive effect in combination). Therefore, they are more potent in the presence of TRAIL than in its absence. Maritinone (**4**) and elliptinone (**5**) showed the highest degree of TRAIL sensitization, as their synergistic effects were more than 3-fold greater than the compounds alone. 2,3-Epoxy-2,3-dihydro-8-
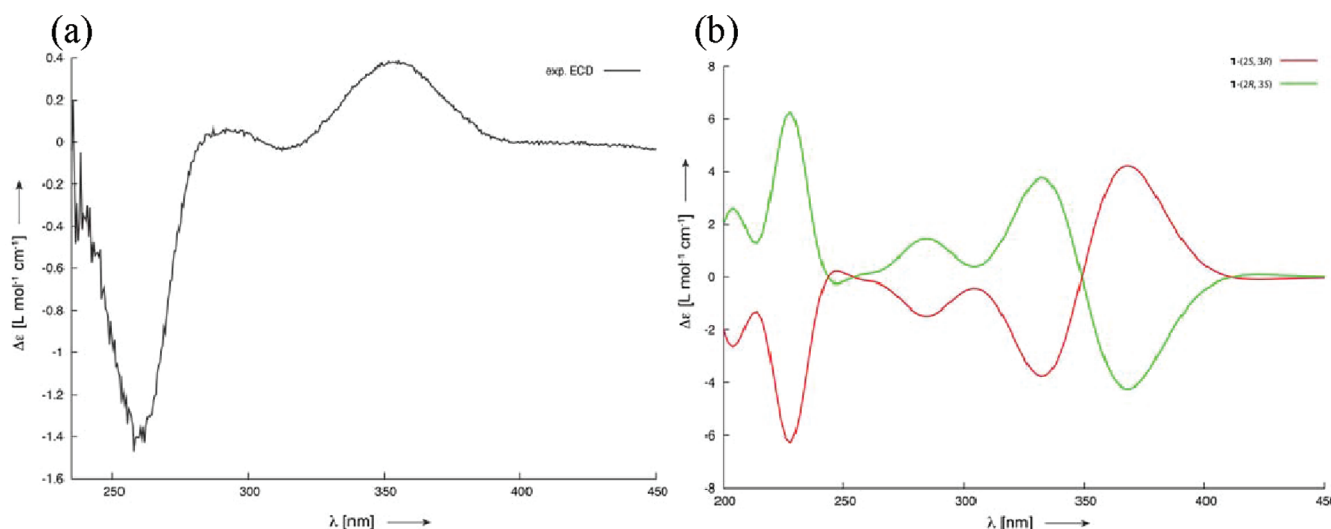
Figure 3. Comparison of (a) experimental ECD values with (b) those calculated for the two possible enantiomers (2S,3R and 2R,3S) of **1**. The calculations were performed with DFT at the B3LYP/6-31G(d) level using the IEFPCM solvent continuum model with methanol as the solvent. The calculated ECD values are weighted based on the Gibbs free energy.

Table 3. Biological Effects of 1−8 with and without TRAIL

compound	EC$_{50}$^{a} w/ TRAIL^b	EC$_{50}$^{a} w/o TRAIL	synergistic effect^c
2,3-epoxy-2,3-dihydrolapachol (**1**)	16.7	39.7	2.4
2,3-epoxy-2,3-dihydro-8-hydroxylapachol (**2**)	4.7	6.4	1.4
2-methylanthraquinone (**3**)	>50	>50	NA
maritinone (**4**)	1.5	5.8	3.8
elliptinone (**5**)	3.8	13.2	3.5
plumbagin (**6**)	3.7	7.3	2.0
(+)-cis-isoshinanolone (**7**)	>60	>60	NA
ethylidene-6,6′-biplumbagin (**8**)	>30	>30	NA

^{a}μM. ^{b}40 ng/mL. ^{c}Synergistic effect is defined as the ratio of the two half-maximal (EC$_{50}$) values obtained from cell death curves.

hydroxylapachol (**2**) was a more potent cytotoxic agent than 2,3-epoxy-2,3-dihydrolapachol (**1**); however, **1** showed a higher synergistic effect with TRAIL. Interestingly, 2-methylanthraquinone (**3**), (+)-cis-isoshinanolone (**7**), and ethylidene-6,6′-biplumbagin (**8**) were not cytotoxic, despite their structural similarities to the active compounds.

In summary, 2,3-epoxy-2,3-dihydrolapachol (**1**), 2,3-epoxy-2,3-dihydro-8-hydroxylapachol (**2**), and 2-methylanthraquinone (**3**) were isolated from *B. alluaudii*. Neither **1** nor **2** has been reported previously from natural sources, and the absolute configuration of **1** and **2** was determined using TD-DFT calculations of ECD spectra. Additionally, five known compounds were isolated from *D. maritima* (**4**−**8**). Compounds **1**, **2**, and **4**−**6** showed TRAIL sensitization, and compounds **4** and **5** showed more than three times the effect with TRAIL than without. No previous investigations of *B. alluaudii*, endemic to Madagascar, have been reported in the chemical literature. Compounds **1** and **2** are members of the lapachol family of quinones. β-Lapachol was evaluated by the NCI in the clinic during the 1970s, but was later withdrawn due to high levels of toxicity.[34] The closely related β-lapachone is currently in phase II clinical trials for advanced solid tumors.[34,35]

EXPERIMENTAL SECTION

General Experimental Procedures. Optical rotations were measured on a Perkin-Elmer 241 polarimeter. UV spectra were acquired in spectroscopic grade MeOH using a Varian Cary 50 UV−vis spectrophotometer. ECD spectra were recorded on a JASCO J-720 spectropolarimeter or an AVIV 202. NMR data were collected using a Bruker Avance III DRX-600 (^{1}H 600 MHz, ^{13}C 150 MHz) NMR spectrometer (Bruker Biospin) with a 3 mm CPTCI probe, referenced to residual solvent (δ_H 7.24, δ_C 77.23 for CDCl$_3$; δ_H 3.31, δ_C 49.15 for CD$_3$OD). MS were measured with an Agilent Technologies 6510 Q-TOF LC-MS and an Applied Biosystems, Inc. QSTAR XL hybrid triple-quad time-of-flight (QqTOF) mass spectrometer. Initial purification was performed on Diol SPE cartridges (Applied Separations) and Sephadex LH-20 resin (Amersham Biosciences). All HPLC was performed on a Rainin SD-1/UV-1 system utilizing a Rainin Dynamax C$_{18}$ column (250 × 10 mm, 5 μm particle size) at 4.5 mL/min.

Plant Material. The stems of *Barleria alluaudii* Benoist (Acanthaceae) were collected approximately 60 km west of Fort-Dauphin, Toliara, Madagascar (24 59.00 S; 46 33.00 E) by J. Zarucchi, E. Rakotobe, A. Randrianasolo, and A. Pool (May 24, 1991). The plant was identified by J. Zarucchi, and a voucher specimen (collection number Q66 V600) is maintained at the Missouri Botanical Garden.

The fruits of *Diospyros maritima* Blume (Ebenaceae) were collected on the Ujung Kulon Reserve, Handeleum Island (Timor) near Java, Indonesia (6 12.00 S; 105 26.00 E), by A. McDonald and Afriastini (May 23, 1992). The plant was identified by A. McDonald, and a voucher specimen (collection number U44Z4517) is maintained at the Field Museum, Chicago, Illinois.

Extraction and Isolation. The stems of *B. alluaudii* (1.192 kg) were extracted successively with CH$_2$Cl$_2$−MeOH (1:1) and MeOH.[36] The combined extracts were reduced to dryness in vacuo to give 49.04 g of crude extract. A portion of this extract (203.6 mg) was separated by two Diol SPE cartridges (2 g resin each), and the equivalent fractions were combined to give five total fractions (74A−74E): fraction A = 9:1 hexanes−CH$_2$Cl$_2$, fraction B = 20:1 CH$_2$Cl$_2$−EtOAc, fraction C = EtOAc, fraction D = 5:1 EtOAc−MeOH, fraction E = MeOH. Size-exclusion chromatography of the active fraction 74A on Sephadex LH-20 (2.5 × 70 cm) using hexanes−CH$_2$Cl$_2$−MeOH (2:5:1) yielded 11 fractions (90A−90K). Fraction 90D was separated further by Sephadex LH-20 (0.75 × 50 cm) using CH$_2$Cl$_2$−MeOH (1:1) to yield six fractions (110A−110F). Fraction 110D and 110E were purified by HPLC employing an isocratic method of 75% CH$_3$CN−25% H$_2$O (+0.1% AcOH) over 15 min to yield 2,3-epoxy-2,3-dihydro-8-hydroxylapachol (**2**, 8.5 mg) and 2-methylanthraqui-

none (**3**, 0.9 mg). Fractions 110B and 110C were purified by HPLC employing a gradient of 60% CH$_3$CN−40% H$_2$O (+0.1% AcOH) to 95% CH$_3$CN over 20 min to yield 2,3-epoxy-2,3-dihydrolapachol (**1**, 4.1 mg) and **2** (4.4 mg).

The fruits of *D. maritima* (0.756 kg) were extracted successively with CH$_2$Cl$_2$−MeOH (1:1) and MeOH.[36] The combined extracts were reduced to dryness in vacuo to give 24.3 g of crude extract. A portion of this extract (199.3 mg) was separated by two Diol SPE cartridges (2 g of resin each) to give five total fractions (75A−75E), as highlighted above. Size-exclusion chromatography of active fraction 75B on Sephadex LH-20 (2.5 × 70 cm) using hexanes−CH$_2$Cl$_2$−MeOH (2:5:1) yielded (+)-*cis*-isoshinanolone (**7**, 3.2 mg) and nine other fractions (78A−78G, 78I, and 78J). Fractions 78D and 78E were purified by HPLC employing a gradient of 60% CH$_3$CN−40% H$_2$O (+0.1% AcOH) to 100% CH$_3$CN over 20 min to yield elliptinone (**5**, 1.1 mg). Size-exclusion chromatography of active fraction 75A on Sephadex LH-20 (2.5 × 70 cm) using hexanes−CH$_2$Cl$_2$−MeOH (2:5:1) yielded plumbagin (**6**, 42.4 mg) and seven other fractions (89A−89F and 89H). Fraction 89E was purified by HPLC employing a gradient of 60% CH$_3$CN−40% H$_2$O (+0.1% AcOH) to 90% CH$_3$CN over 20 min to yield maritinone (**4**, 1.2 mg).

A larger portion of the extract (1.0 g) was separated on a Diol column (2.0 × 5.5 cm, 10 g resin) to give five total fractions (130A−130E), as highlighted above. Size-exclusion chromatography of fraction 130A on Sephadex LH-20 (2.5 × 70 cm) using hexanes−CH$_2$Cl$_2$−MeOH (2:5:1) yielded eight fractions (159A−159H). Fractions 159B−159D were combined and separated further by Sephadex LH-20 (0.75 × 50 cm) using CH$_2$Cl$_2$−MeOH (1:1) to yield six fractions (168A−168F). Fractions 168D and 168E were purified employing the gradient utilized to purify elliptinone to yield ethylidene-6,6′-biplumbagin (**8**, 0.7 mg).

(2*S*,3*R*)-2,3-Epoxy-2,3-dihydrolapachol (1): $[\alpha]^{25}_D$ −9.0 (*c* 0.2, MeOH); UV (MeOH) λ_{max} (log ε) 304 (3.22) 263 (3.79) 228 (4.42) nm; ^{1}H NMR and ^{13}C NMR data, see Table 1; HRESIMS *m/z* 243.1020 [M + H]$^+$ (calcd for C$_{15}$H$_{15}$O$_3$, 243.1016).

(2*S*,3*R*)-2,3-Epoxy-2,3-dihydro-8-hydroxylapachol (2): $[\alpha]^{25}_D$ +92.8 (*c* 0.2, MeOH); UV (MeOH) λ_{max} (log ε) 360 (3.88) 262 (3.66) 233 (4.26) 206 (4.28) nm; ^{1}H NMR and ^{13}C NMR data, see Table 1; HRESIMS *m/z* 259.0966 [M + H]$^+$ (calcd for C$_{15}$H$_{15}$O$_4$, 259.0965).

Conformational Analysis, Geometry Optimization, ECD, and ORD Calculations. The initial structures of **1** and **2** were built with Discovery Studio 2.5 (Accelrys), and all trial structures were first minimized based on molecular mechanics calculations (CFF force field[37]). To sample the conformational space, a conformational search was performed (BEST method in Discovery Studio 2.5) based on molecular mechanics calculations (CFF force field). Conformers occurring within a 10 kcal/mol energy window from the global minimum were chosen for geometry optimization and energy calculation using DFT[19,20] with the B3LYP functional and the 6-31(d) basis set with the Gaussian09 program.[38] TD-DFT[19,20] with the basis set B3LYP/631G(d) was used to calculate the spin-allowed excitation energies and rotatory (R_n) and oscillator strengths (f_n) of the lowest 50 excited states. The spectra were combined after Boltzmann weighting according to their population contribution. The optical rotation dispersion calculations at the three wavelengths 546, 578, and 589 nm were performed with the optimized structures as input coordinates with the same basis set as the geometry optimization and ECD calculations. All the calculations were performed in vacuo with the integral equation formalism variant polarizable continuum model as implemented in Gaussian 09 (methanol as solvent).

TRAIL Assay. The biological activity of each extract, chromatographic fraction, or pure compound was monitored using the screening assay described previously.[5] Briefly, ACHN cell numbers were assessed after 20−24 h treatment with varying concentrations of extract, fraction, or pure compound in the absence or presence of 40 ng/mL TRAIL. TRAIL has no effect on ACHN cells up to 10 ug/mL. Bortezomib at 40 nM (final concentration) was used as the positive control.

ASSOCIATED CONTENT

S **Supporting Information**

^{1}H and ^{13}C NMR spectra for **1** and **2**, chiral HPLC analysis of **1**, Gaussian keywords, calculated excitation energies, oscillator strengths, and rotational strengths for **1** and **2**, important dihedral angles of conformers **1a−1f** and **2a−2f**, conformational analysis of **1**, calculated ORD values for **1** and **2**, and coordinates of conformers **1a−1f** and **2a−2f** . This material is available free of charge via the Internet at http://pubs.acs.org.

AUTHOR INFORMATION

Corresponding Author
*Tel: (301) 846-1943. Fax: (301) 846-6851. E-mail: mckeeta@mail.nih.gov.

Notes
The authors declare no competing financial interest.

DEDICATION

Dedicated to Dr. Gordon M. Cragg, formerly Chief, Natural Products Branch, National Cancer Institute, Frederick, Maryland, for his pioneering work on the development of natural product anticancer agents.

REFERENCES

(1) Mahalingam, D.; Szegezdi, E.; Keane, M.; Jong, S.; Samali, A. *Cancer Treat. Rev.* **2009**, *35*, 280−288.
(2) MacFarlane, M.; Williams, A. C. *EMBO Rep.* **2004**, *5*, 674−678.
(3) Mahmood, Z.; Shukla, Y. *Exp. Cell Res.* **2010**, *316*, 887−899.
(4) Sayers, T. J. *Cancer Immunol. Immunother.* **2011**, *60*, 1173−1180.
(5) Booth, N. L.; Sayers, T. J.; Brooks, A. D.; Thomas, C. L.; Jacobsen, K.; Goncharova, E. I.; McMahon, J. B.; Henrich, C. J. *Cancer Immunol. Immunother.* **2009**, *58*, 1229−1244.
(6) Zhang, L.; Fang, B. *Cancer Gene Ther.* **2005**, *12*, 228−237.
(7) Van Geelen, C. M.; de Vries, E. G.; de Jong, S. *Drug Resist. Updates* **2004**, *7*, 345−358.

(8) O'Kane, H. F.; Watson, C. J.; Johnston, S. R.; Petak, I.; Watson, R. W.; Williamson, K. E. *J. Urol.* **2006**, *175*, 432−438.

(9) Cheng, J.; Hylander, B. L.; Baer, M. R.; Chen, X.; Repasky, E. A. *Mol. Cancer Ther.* **2006**, *5*, 1844−1853.

(10) Huang, Y.; Sheikh, M. S. *Toxicol. Appl. Pharmacol.* **2007**, *224*, 284−289.

(11) Duiker, E. W.; Mom, C. H.; de Jong, S.; Willemse, P. H.; Gietema, J. A.; van der Zee, A. G.; de Vries, E. G. *Eur. J. Cancer* **2006**, *42*, 2233−2240.

(12) Buchsbaum, D. J.; Forero-Torres, A.; LoBuglio, A. F. *Future Oncol.* **2007**, *3*, 405−409.

(13) Whitson, E. L.; Thomas, C. L.; Henrich, C. J.; Sayers, T. J.; McMahon, J. B.; McKee, T. C. *J. Nat. Prod.* **2010**, *73*, 2013−2018.

(14) Claessens, S.; Habonimana, P.; De Kimpe, N. *Org. Biomol. Chem.* **2010**, *8*, 3790−3795.

(15) Preusch, P. C.; Suttie, J. W. *J. Org. Chem.* **1983**, *48*, 2291−2293.

(16) Pluim, H.; Wynberg, H. *J. Org. Chem.* **1980**, *45*, 2498−2502.

(17) Perry, N. B.; Blunt, J. W.; Munro, M. H. *J. Nat. Prod.* **1991**, *54*, 978−985.

(18) Matsumoto, T.; Ichihara, A.; Yanagiya, M.; Yuzawa, T.; Sannai, A.; Oikawa, H.; Sakamura, S.; Eugster, C. H. *Helv. Chim. Acta* **1985**, *68*, 2324−2331.

(19) Di Bari, L.; Guillarme, S.; Hermitage, S.; Jay, D. A.; Pescitelli, G.; Whiting, A. *Chirality* **2005**, *17*, 323−331.

(20) Furche, F.; Ahlrichs, R.; Wachsmann, C.; Weber, E.; Sobanski, A.; Vogtle, F.; Grimme, S. *J. Am. Chem. Soc.* **2000**, *122*, 1717−1724.

(21) Sun, H.; d'Auvergne, E. J.; Reinscheid, U. M.; Dias, L. C.; Andrade, C. K.; Rocha, R. O.; Griesinger, C. *Chem.—Eur. J.* *17*, 1811−1817.

(22) Stephens, P. J.; McCann, D. M.; Cheeseman, J. R.; Frisch, M. J. *Chirality* **2005**, *17*, S52−S64.

(23) McCann, D. M.; Stephens, P. J. *J. Org. Chem.* **2006**, *71*, 6074−6098.

(24) Kafuku, K.; Sebe, K. *Bull. Chem. Soc. Jpn.* **1932**, *7*, 114−127.

(25) Rath, G.; Ndonzao, M.; Hostettmann, K. *Int. J. Pharmacogn.* **1995**, *33*, 107−114.

(26) Tezuka, M.; Takahashi, C.; Kuroyanagi, M.; Satake, M.; Yoshihira, K.; Natori, S. *Phytochemistry* **1973**, *12*, 175−183.

(27) Gu, J. Q.; Graf, T. N.; Lee, D.; Chai, H. B.; Mi, Q.; Kardono, L. B.; Setyowati, F. M.; Ismail, R.; Riswan, S.; Farnsworth, N. R.; Cordell, G. A.; Pezzuto, J. M.; Swanson, S. M.; Kroll, D. J.; Falkinham, J. O.; Wall, M. E.; Wani, M. C.; Kinghorn, A. D.; Oberlies, N. H. *J. Nat. Prod.* **2004**, *67*, 1156−1161.

(28) Fallas, A. L.; Thomson, R. H. *J. Chem. Soc. C* **1968**, 2279−2282.

(29) Zakaria, M. B.; Jeffreys, J. A. D.; Waterman, P. G.; Zhong, S. M. *Phytochemistry* **1984**, *23*, 1481−1484.

(30) d'Astafort, D. *J. Pharm. Chim.* **1828**, *14*, 441.

(31) Bringmann, G.; Messer, K.; Saeb, W.; Peters, E. M.; Peters, K. *Phytochemistry* **2001**, *56*, 387−391.

(32) Higa, M. *Chem. Pharm. Bull.* **1988**, *36*, 3234−3236.

(33) Higa, M.; Ogihara, K.; Yogi, S. *Chem. Pharm. Bull.* **1998**, *46*, 1189−1193.

(34) Cragg, G. M.; Grothaus, P. G.; Newman, D. J. *Chem. Rev.* **2009**, *109*, 3012−43.

(35) Ravelo, A. G.; Estevez-Braun, A.; Chavez-Orellana, H.; Perez-Sacau, E.; Mesa-Siverio, D. *Curr. Top. Med. Chem.* **2004**, *4*, 241−265.

(36) McCloud, T. G. *Molecules* **2010**, *15*, 4526−4563.

(37) Lifson, S.; Warshel, A. *J. Chem. Phys.* **1968**, *49*, 5116−5129.

(38) Frisch, M. J.; Trucks, G. W.; Schlegel, H. B.; Scuseria, G. E.; Robb, M. A.; Cheeseman, J. R.; Scalmani, G.; Barone, V.; Mennucci, B.; Petersson, G. A.; Nakatsuji, H. *Gaussian 09*, Revision A.1; Gaussian, Inc.: Wallingford, CT, 2009.